BJP British Journal of Pharmacology

DOI:10.1111/j.1476-5381.2011.01804.x
www.brjpharmacol.org

RESEARCH PAPER

Ethyl pyruvate promotes spinal cord repair by ameliorating the glial microenvironment

Yimin Yuan*, Zhida Su*, Yingyan Pu, Xiujie Liu, Jingjing Chen, Feng Zhu, Yanling Zhu, Han Zhang and Cheng He

Institute of Neuroscience and MOE Key Laboratory of Molecular Neurobiology, Neuroscience Research Center of Changzheng Hospital, Second Military Medical University, Shanghai, China

Correspondence
Corresponding author: Cheng He, Institute of Neuroscience and MOE Key Laboratory of Molecular Neurobiology, Neuroscience Research Center of Changzheng Hospital, Second Military Medical University, Shanghai 200433, China. E-mail: chenghe@smmu.edu.cn

*These authors contributed equally to this work.

Keywords
ethyl pyruvate; astrogliosis; neuroinflammation; glial scar; spinal cord injury; axon regeneration

Received
27 June 2011
Revised
22 November 2011
Accepted
29 November 2011

BACKGROUND AND PURPOSE
Spinal cord injury (SCI) triggers a series of endogenous processes, including neuroinflammation and reactive astrogliosis, which may contribute to the failure of neural regeneration and functional recovery. In the present study, the effect of ethyl pyruvate on spinal cord repair was explored.

EXPERIMENTAL APPROACH
Functional assessment and histological analyses of astrogliosis, neuroinflammation, neuronal survival and axonal regeneration were performed to investigate the effects of ethyl pyruvate (0.086, 0.215, 0.431 or 0.646 mmol·kg^{-1}·day^{-1}) on spinal cord repair in a rat model of SCI. The effect of ethyl pyruvate (5, 10 or 15 mM) on astrocytic activation was also evaluated in an *in vitro* 'scratch-wound' model.

KEY RESULTS
Functional assessment showed evident improvement of behavioural functions in the ethyl pyruvate-treated rats. Reactive astrogliosis was significantly inhibited *in vivo*, after injection of ethyl pyruvate (0.431 mmol·kg^{-1}day^{-1}), and *in vitro* 'scratch-wound' model in the presence of 10 or 15 mM ethyl pyruvate. The difference between effective concentration *in vitro* and *in vivo* suggests that the inhibitory effect of ethyl pyruvate on astrogliosis in damaged spinal cord is indirect. In addition, ethyl pyruvate (0.431 mmol·kg^{-1}day^{-1}) attenuated SCI-induced neuroinflammation; it decreased the Iba-1-, ED-1- and CD11b-positive cells at the lesion site. Importantly, histological analyses showed a significantly greater number of surviving neurons and regenerative axons in the ethyl pyruvate-treated rats.

CONCLUSIONS AND IMPLICATIONS
Ethyl pyruvate was shown to inhibit astrogliosis and neuroinflammation, promote neuron survival and neural regeneration, and improve the functional recovery of spinal cord, indicating a potential neuroprotective effect of ethyl pyruvate against SCI.

Abbreviations
AR, angle of rotation; BBB, Basso–Beattie–Bresnehan locomotor score; CSPG, chondroitin sulfate proteoglycans; CST, corticospinal tract; ILC, interlimb coordination; ROS, reactive oxygen species; SCI, spinal cord injury; SL, stride length

Introduction

Although extensive progress has been made on spinal cord injury (SCI) repair in animal models and humans, so far, no satisfactory treatment is currently available. SCI leads to complex cellular and molecular interactions, including primary insult and secondary injury, within the spinal cord in an attempt to repair the initial tissue injury. Traumatic SCI triggers a series of reactive changes, including reactive astrogliosis and inflammatory cell activation, which results in the formation of a degenerative microenvironment in the lesion site. In many studies, this hostile environment, as well as the intrinsic incapacity of the neuron to regenerate, is regarded as an important contributor to the failure of spontaneous anatomical and functional repair of SCI (Fleming *et al.*, 2006; Yiu and He, 2006).

The importance of the glial cell response to injury has been extensively illustrated in the wound-healing processes after CNS injury. Astrocytes are a type of multifunctional cell. Apart from playing an essential homeostatic role and contributing to information processing in physiological conditions, they are also able to respond to various kinds of CNS insult, including physical, chemical, and pathological trauma. In reaction to injury, astrocytes are activated and referred to as reactive astrocytes, resulting in so-called reactive astrogliosis. Reactive astrogliosis is characterized by hyperplasia, hypertrophy of cell bodies and cytoplasmic processes, and up-regulation of intermediate filament proteins [such as glial fibrillary acidic protein (GFAP) and vimentin], and ultimately form a histologically apparent glial scar at the lesion site in the damaged spinal cord (Pekny and Nilsson, 2005; Sofroniew, 2009). In the early phase after CNS injury, glial scar plays a key role in sealing the lesion site, restoring homeostasis, preserving spared tissue and modulating immunity (Okada *et al.*, 2006; Herrmann *et al.*, 2008; Rolls *et al.*, 2009). However, excessive scar formation is one of the major current obstacles of axonal regeneration and functional recovery in the later periods (Yiu and He, 2006). Besides the historical perspective that glial scar constitutes a mechanical barrier to regeneration, it also chemically inhibits SCI repair by releasing inhibitory extracellular matrix molecules, such as chondroitin sulfate proteoglycans (CSPG), tenascin and semaphorin 3 (Fitch and Silver, 2008). Unlike myelin-associated inhibitory molecules that remain at largely static levels before and after CNS damage, these inhibitory extracellular matrix molecules in glial scar are dramatically increased during the inflammatory stages after injury, which provides a window of opportunity for therapeutic interventions. Importantly, some strategies designed to modify reactive astrogliosis and glial scar formation have been found to promote axonal regeneration and functional recovery after adult CNS injury (Goldshmit *et al.*, 2004; Wilhelmsson *et al.*, 2004; Tian *et al.*, 2007).

An additional important influencing factor involved in the abortive attempts of neuronal regeneration after SCI is the inflammatory cell activation. Immune cells play a critical role in the resolution of wound healing and pathologies that occur in peripheral organs. Although the CNS had been considered immune privileged, neuroinflammation is now recognized as a typical hallmark of both acute and chronic neurodegenerative disease. Following CNS injury, an intensive local inflammatory response is observed, involving activation of resident microglia in the CNS and coordinated infiltration of the damaged site by various leucocytes from the peripheral blood (Popovich and Hickey, 2001; Stoll *et al.*, 2002; Fleming *et al.*, 2006). Interestingly, it has been shown that the acute inflammatory response to traumatic injury is greater in the spinal cord than in the cerebral cortex (Schnell *et al.*, 1999). The SCI-induced cellular inflammatory response has been implicated as one mechanism of secondary damage at the injury site and in lesion extension into nearby rostral/caudal spinal levels (Dusart and Schwab, 1993; Popovich *et al.*, 1997; Fleming *et al.*, 2006). While high-dose methylprednisolone steroid therapy alone has not proved to be the solution to this problem, other strategies for modulating neuroinflammation are providing robust evidence for alleviating axonal damage and improving neurological function (Cuzzocrea *et al.*, 2008; Tederko *et al.*, 2009; Tian *et al.*, 2009).

As the final product of glycolysis and the substrate for the tricarboxylic acid cycle, pyruvate plays a key role in intermediary metabolism (Vander Heiden *et al.*, 2009). In addition, pyruvate has also been reported to be an effective scavenger of reactive oxygen species (ROS) in cells (Jagtap *et al.*, 2003; Hinoi *et al.*, 2006; Wang *et al.*, 2007) and an anti-inflammatory agent (Gupta *et al.*, 2000; Das, 2006; Wang *et al.*, 2009). However, its poor stability in solution may limit the usefulness of pyruvate as a therapeutic agent (von Korff, 1964). Ethyl pyruvate is a stable and lipophilic derivative of endogenous pyruvate (Sims *et al.*, 2001; Fink, 2003; 2007), and, along with pyruvate or ethyl pyruvate has been shown to ameliorate organ injury or dysfunction in a wide variety of animal models, including haemorrhagic shock (Mongan *et al.*, 2001), transient cerebral ischaemia (Lee *et al.*, 2001; Yu *et al.*, 2005; Tokumaru *et al.*, 2009; Shen *et al.*, 2010), traumatic brain injury (Moro and Sutton, 2010) and Parkinson's disease (Choi *et al.*, 2010; Huh *et al.*, 2011).

In the current study, we explored the effect of ethyl pyruvate on the damaged spinal cord using a rat model of SCI. Administration of ethyl pyruvate was shown to inhibit astrogliosis and neuroinflammation, promote neuron survival and neural regeneration, and improve the functional recovery of spinal cord, indicating a potent neuroprotective effect of ethyl pyruvate against SCI.

Methods

SCI and experimental groups

Adult male Sprague-Dawley rats (170–200 g) were used for the SCI study. The animals were housed at a constant temperature of 22°C on a 12-hour light/dark cycle with access to food and water *ad libitum*. All animal care and experimental procedures complied with the guidelines recommended by the National Institutes of Health for the care and use of animals for scientific purposes and were approved by the Animal Experimentation Ethics Committee of the Second Military Medical University.

Spinal cord hemisection at T8 was performed as previously described with slight modifications (Vavrek *et al.*, 2006). Animals were anaesthetized with 2% pentobarbital sodium (40 mg kg^{-1}). The analgesia was assessed as the

absence of response to a toe-web pinch. Laminectomy was performed to expose the dorsal surface of the T7–9 segment, followed by a spinal right hemisection at T8 using a fine corneal blade (cut twice in the same place to ensure complete section). Post-operatively, animals were kept at 22–25°C on highly absorbent bedding, and received manual bladder expression twice daily until reflexive bladder control returned. Rats were randomly divided into three experimental groups: (i) sham-operated group (sham), in which the spinal cord was exposed but not lesioned; (ii) injured-control group (control), which received SCI with no ethyl pyruvate but an i.p. injection of normal saline solution; and (iii) ethyl pyruvate-treated group (ethyl pyruvate), which received SCI with ethyl pyruvate in normal saline by i.p. injection.

Functional assessment

All behavioural assessments were performed by observers unaware of (blinded to) the experimental groups. Firstly, the Basso–Beattie–Bresnehan (BBB) locomotor score was used to rate hindlimb movements following SCI as previously described (Basso *et al.*, 1995) 1, 7, 14, 21, 28 and 35 days after operation. In brief, the rats were placed individually in an open field with a non-slippery surface where one animal at a time was allowed to move freely for 5 min. A BBB scale, in which a score of 21 was considered normal and a score of zero indicated no hindlimb movement, was used to assess hindlimb locomotor recovery including joint movements, stepping ability, coordination, and trunk stability.

Secondly, the rung horizontal-ladder test was used to assess the deficits in the descending motor functions (Karimi-Abdolrezaee *et al.*, 2006). The rung ladder that consisted of a 1 m long tunnel containing a ladder with rungs 0.5 cm in diameter was elevated 30 cm from the ground, where the ability of animals to walk on it was evaluated. This test requires the rat to be able to coordinate hindlimb movements with forelimb movements in order that the hindlimbs do not slip through the gaps between the rungs. To assess the deficits in the descending motor functions, the ability of rats to walk on the horizontal ladder with metal rungs was assessed 14, 21, 28 and 35 days after operation. For quantitative purposes, the number of foot slips of each rat was counted during a period where they were allowed to walk freely on the horizontal grid. Before SCI or sham surgery, rats were trained for three sessions. For each session, the average number of foot falls of each animal was taken from three trials. The number of foot slips counted in the control group and in the ethyl pyruvate-treated group was normalized to that counted in sham-operated group.

Finally, locomotor activity was also evaluated using the foot-print analyses system following the previous protocols (Karimi-Abdolrezaee *et al.*, 2006). Animals that could support their own weight were footprinted by dipping their forelimbs and hindlimbs in red and black non-toxic ink, respectively. Then, the foot-printed rats were allowed to walk across a narrow runway covered with white paper (1 m length and 7 cm width). To prevent the rats from pausing while passing the track, a very bright box and a dark box with food was placed at the beginning and at the end of the runway, respectively. The footprints of rats were analysed before the operation and 14, 21, 28 and 35 days after the operation by measuring the stride length (SL, determined by measurement of multiple successive steps), angle of rotation (AR, the angle made by two lines connecting the third toe and the stride line at the centre of the paw pad) and interlimb coordination (ILC, the distance between the centre pads of the ipsilateral forelimb and hindlimb) where SL, AR and ILC were indicated as a percentage of each rat's own baseline, measured before the operation.

Analyses of astrogliosis in vivo

Histological analyses of astrocytic gliosis *in vivo* were performed as previous protocols (Su *et al.*, 2010). The spinal cord-hemisected rats were injected (i.p.) with 0.431 mmol·kg^{-1} day^{-1} ethyl pyruvate or normal saline solution. This treatment was initiated immediately after spinal cord hemisection and continued at regular intervals for a total of 10 doses. Ten days later, the animals were killed by injection with an overdose of pentobarbital sodium and a 1.5 cm length of the spinal cord spanning the lesion site was isolated from the killed rats. Serial longitudinal sections (10 μm) were cut in the horizontal plane and every fifth section was collected. After immunofluorescent staining with GFAP, the size, the total number and the fluorescent intensity of GFAP-positive cells were counted in a 0.25 mm^2 grid close to or 1 mm proximal to the lesion site to quantify the reactive astrogliosis in the damaged spinal cord. In addition, detection of the CSPG-positive region, a fundamental component of glial scar, can be used to quantitatively assess the formation of glial scar after SCI. Rats from the control group and the ethyl pyruvate group were treated with normal saline or ethyl pyruvate from day 0 to day 10. Four weeks after SCI, the size and the fluorescent intensity of the CSPG-positive area was measured in every fifth horizontal section centered at the injury sites to quantitatively evaluate the glial scar formation in the injured spinal cord.

Primary astrocyte cultures

Highly enriched primary astrocytes were isolated from the cerebral cortex of 2 day-old newborn Sprague-Dawley rat as previously described (Cao *et al.*, 2007). After removal of the meninges, the cerebral cortices were dissociated into a single-cell suspension by trypsinization and mechanical disruption. The cells were seeded on poly-L-lysine- (PLL, 0.1 mg·mL^{-1}; Sigma, St Louis, MO, USA) coated culture flasks and incubated in Dulbecco's modified Eagle's medium/F-12 containing 10% fetal calf serum. After 8–10 days, an enriched astrocyte culture was obtained from this mixture of glial cells by shaking the flasks on a rotary shaker at 260 r.p.m. for 18–20 h at 37°C to remove microglia and oligodendrocyte precursor cells. Astrocytes were subsequently detached using trypsin-EDTA and plated into PLL-coated 12-well plates or onto PLL-coated cover slips. The cultures routinely contained > 98% astrocytes, as assessed by expression of the astrocyte marker GFAP.

In vitro *astrocytic activation model*

Cultured astrocytes were activated by scratch injury as previously reported (Yu *et al.*, 1993). Briefly, astrocytes were plated in PLL-coated 12-well plates. Upon growing to confluence, the astrocyte monolayers were scratched with a sterile 200 μL plastic pipette tip to form a cell-free area approximately

1 mm wide. After cultures were washed twice with sterile PBS to remove detached cells, the medium was replaced with Neurobasal-B27 medium. To test the effect of ethyl pyruvate on astrogliosis *in vitro*, astrocytes were stimulated with 5, 10 or 15 mM ethyl pyruvate (dissolved in Neurobasal-B27 medium).

Cell proliferation assay

Cell proliferation was assessed by the 5-bromo-2-deoxyuridine (BrdU) incorporation assay as described previously (Su *et al.*, 2010). After treatment with or without ethyl pyruvate for 24 h, 10 μM BrdU (Sigma) was administered to the cultures for the last 18 h before immunostaining. Astrocytes were fixed with 4% paraformaldehyde (PFA) for 20 min, followed by treatment with 2 N HCl for 10 min to denature DNA, and then 0.1 M sodium borate (pH 8.5) for 10 min to neutralize the acid. BrdU incorporation was detected by fluorescent staining using an anti-BrdU monoclonal antibody (Thermo Scientific, Waltham, MA, USA). Hoechst labelling was used to image the nuclei. Cell proliferation index was determined as the ratio of $BrdU^+$ cells to $Hoechst^+$ cells.

Immunostaining

For immunocytochemical analyses, astrocytes in 12-well plates or on coverslips were fixed with 4% PFA for 20 min and permeabilized with 0.3% Triton X-100 in 0.1 M PBS, followed by blocking the non-specific binding in PBS containing 10% goat serum. Then, cells were incubated with primary antibodies against GFAP (Sigma) or Vimentin (Boster, Wuhan, China) overnight at 4°C. After being washed three times in PBS, cultures were incubated with appropriate fluorescence-conjugated secondary antibodies (Jackson ImmunoResearch Laboratories Inc., West Grove, PA, USA) for 90 min at room temperature. Cells were viewed and photographed with an Olympus BX70 fluorescence microscope (Olympus, Center Valley, PA, USA).

For immunohistochemical analyses, animals were deeply anaesthetized with 2% pentobarbital sodium and perfused transcardially with 4% PFA in 0.1 M PBS. The spinal cords were subsequently dissected from each animal and post-fixed in the perfusing solution overnight at 4°C. Then, the tissues were cryoprotected in 20% sucrose in PBS for 24–48 h at 4°C. Cryostat sections (10 μm) were cut and mounted onto gelatin-subbed slides. The slides were permeabilized and blocked with 0.3% Triton X-100/10% normal goat serum in 0.1 M PBS for 15 min. Primary antibodies against GFAP (Sigma), CSPG (Sigma), Iba-1 (Abcam Ltd, Cambridge, UK), ED-1 (Millipore, Billerica, MA, USA) or CD11b (Boster) were then applied to the sections overnight at 4°C. The following day, sections were incubated with fluorescence-conjugated secondary antibodies (Jackson ImmunoResearch Laboratories Inc.) and examined by Olympus fluorescence microscopy. All histological analysis was performed by observers unaware of (blinded to) the experimental groups.

Western blot

Changes in protein expression of GFAP *in vitro* and *in vivo* were analysed by Western blot. The cell or tissue lysates were denatured by boiling for 10 min and then centrifuged for 10 min at 13,000x*g* at 4°C. Proteins were separated by SDS-polyacrylamide gel and then transferred onto nitrocellulose membranes. Membranes were then blocked with 10% non-fat milk in 1 × tris buffered saline with Tween and incubated with primary antibodies against GFAP (Sigma). To control for differences in protein loading, membranes were also incubated with anti-GAPDH antibody (Sigma). After incubating with horseradish peroxidase-conjugated secondary antibodies (Sigma), immunoreactive bands were visualized by chemiluminescence reagents (Amersham ECL; Amersham Pharmacia Biotech, Little Chalfont, Bucks, UK).

Terminal deoxynucleotidyl transferase-mediated 2′-deoxyuridine 5′-triphosphate nick end labeling assay (TUNEL) staining

Programmed cell death *in situ* was analysed by specific labelling of nuclear DNA fragmentation (TUNEL) using the *In Situ* Cell Death Detection Kit (Roche Products, Hertfordshire, UK) according to the manufacturer's instructions. Briefly, the sections prepared as described for immunohistochemistry were immersed in TUNEL reaction mixture and incubated in a humid atmosphere at 37°C for 60 min. The cellular marker NeuN was used to label neurons in the spinal cord. Quantification of cell apoptosis was accomplished by counting the number of TUNEL and NeuN-positive cells under a fluorescence microscope.

Anterograde tracing

To trace endogenous axons, 10% tetramethylrhodamine biotinylated dextran amine (BDA; Molecular Probes, Eugene, OR, USA) was injected into the motor cortex as described previously (Cao *et al.*, 2004; Ruitenberg *et al.*, 2005). After exposure of both sensorimotor cortices by drilling two holes in the cranium, a 10% BDA in sterile PBS was injected bilaterally in eight sites of each sensorimotor cortex (0.5 μL per site) to cover the entire hindlimb region (Figure 7A). Two weeks later, the animals were killed and the spinal cords were dissected. Serial horizontal sections (10 μm) were collected and the signal fluorescence in each section was measured with the Image-Pro Plus image analyses software for quantitative analyses of BDA-labelled corticospinal tract (CST). Background and non-specific labelling in each image was excluded by altering the intensity thresholds. In horizontal sections, the density of BDA-labelled axons running rostrally to caudally through the hemisection was detected in right (ipsilateral to the lesion site) half spinal cord at 1 mm caudal to the lesion site in every fifth section. To control for differences in axon tracing and labelling efficiency between animals, the fluorescent intensities of BDA-labelled axons measured within right half spinal cord were normalized to that detected within left (contralateral to the lesion site) spinal cord for each horizontal section examined.

Statistical analyses

All data are presented as mean ± SD and were compared statistically using Student's unpaired *t*-test or ANOVA with pair-wise comparisons. Statistical significance was defined as $P < 0.05$.

Results

Improvement of hindlimb functions after treatment with ethyl pyruvate

To determine whether treatment with ethyl pyruvate improved recovery of function after SCI, three independent behavioural tasks, including BBB open-field scoring, horizontal-ladder test, and foot-print analyses, were used to assess the behavioural functions.

After i.p. administration of ethyl pyruvate at doses of 0.215, 0.431 or 0.646 mmol·kg^{-1} day^{-1} immediately following SCI, behavioural evaluation by BBB scoring was performed (Figure 1A). In the open field, sham-operated animals obtained a maximum BBB score during the 5-week assessment period. On the first day after SCI, the control and ethyl pyruvate-treated animals manifested complete hindlimb paralysis with no observable hindlimb movement. By 1 week after surgery, although both control and ethyl pyruvate-treated animals had improved hindlimb locomotor function, they did not have significantly different BBB scores. From 2 to 5 weeks after SCI, hindlimb locomotor performance of both control and ethyl pyruvate-treated animals had continued to be improved gradually, but the ethyl pyruvate-treated (0.215, 0.431 or 0.646 mmol·kg^{-1} day^{-1}) group displayed BBB scores greater than that achieved by any of the control animals. Importantly, the 0.431 and 0.646 mmol·kg^{-1} doses of ethyl pyruvate were more effective than the 0.215 mmol·kg^{-1} dose, while there was no significant difference between the effects of ethyl pyruvate at 0.431 and 0.646 mmol·kg^{-1}day^{-1}. In addition, we also investigated the effect of ethyl pyruvate administered at different times after SCI. As shown in Figure 1B, injection of ethyl pyruvate (0.431 mmol·kg^{-1} day^{-1}) immediately or 12 h after SCI was shown to improve hindlimb locomotor function, while no significant improvement was observed when ethyl pryruvate was administered 24 h after SCI.

Ethyl pyruvate-treated animals also performed better on the horizontal-ladder walk task. When rats showed sufficient recovery to bear weight, they were applied to the horizontal-ladder test in which forelimb–hindlimb coordination and voluntary motor movement integration are required to complete the task, walking across a 1 m horizontal grid-way. As shown in Figure 1C, all sham-operated rats accurately accomplished the test with almost no errors in foot placements during the assessment period. By 3 weeks after operation, both control and ethyl pyruvate-treated animals showed significant deficits in hindlimb placements. By 4 weeks after SCI, although a progressive decrease in the number of footfalls was observed in both control and ethyl pyruvate groups, ethyl pyruvate-treated animals had a significantly decreased number of footslips of the hindpaw. Statistical analyses showed that animals in the ethyl pyruvate-treated group had significantly better foot placements at 4 and 5 weeks after SCI, compared with the control SCI group (Figure 1C).

In the footprint test, parameters including SL, AR and ILC were used to analyse the animals' footprint patterns weekly after SCI. As shown in Figure 1D and E, the footprint patterns from sham-operated rats maintained almost 100% of their baseline SL. However, a decreased SL was observed both in control and ethyl pyruvate-treated animals. By 3 weeks after surgery, animals treated with ethyl pyruvate regained a significantly greater SL than that of the SCI control group. Figure 1D and F show a consistent improvement in the AR in hindlimb placement of control and ethyl pyruvate-treated animals. Importantly, rats receiving ethyl pyruvate revealed a more dramatic reduction in hindlimb AR than control animals at 3, 4 and 5 weeks after SCI. The footprint assessments also indicated that the ethyl pyruvate group had a significantly better improvement in ILC, compared with the control group (Figure 1D and G). Taken together, multiple behavioural analyses suggested that treatment of rats with ethyl pyruvate improved locomotor recovery after SCI.

Inhibition of reactive astrogliosis by ethyl pyruvate

To determine whether ethyl pyruvate affected reactive astrogliosis *in vivo*, immunohistochemical analyses were performed in an animal model with spinal cord hemisection. Astroglial hyperplasia is a major property of reactive gliosis in the damaged CNS. As shown in Figure 2A and C, spinal cord hemisection resulted in a significant increase in the total number of GFAP-positive cells close to the lesion (peri-lesion areas) compared with that in distant areas (1 mm proximal to the injury). After treatment of spinal cord-hemisectioned animals with ethyl pyruvate (0.431 mmol·kg^{-1}day^{-1}) for 10 successive days, the number of GFAP immunoreactive cells in peri-lesion areas but not in distant areas was significantly decreased, suggestive of an inhibitory effect of ethyl pyruvate on SCI-induced astroglial hyperplasia (Figure 2A–C). In addition, up-regulation of GFAP was observed in the vast majority of astrocytes in peri-lesion areas; their cell bodies became hypertrophic and extended large and thick processes (Figure 2A). However, treatment with ethyl pyruvate markedly reduced the expression of GFAP (Figure 2A, B and D) and attenuated astrocytic hypertrophy in terms of the average size of GFAP-positive cells (Figure 2A, B and E). Western blot analyses of GFAP expression in spinal cord also indicated that SCI-induced up-regulation of GFAP was significantly attenuated by ethyl pyruvate treatment (Figure 2F).

An *in vitro* 'scratch-wound' model was also used to evoke astroglial responses to mechanical injury and examine whether ethyl pyruvate influences the reactive astrogliosis. Treatment of astrocytes with ethyl pyruvate at a dose of 10 or 15 mM but not 5 mM was shown to ameliorate injury-induced hypertrophy of cell bodies and cytoplasmic processes of astrocytes (Figure 3A). Both GFAP and vimentin participate in the formation of the intermediate filament network. In response to CNS injury, the intermediate filament network becomes very prominent, in particular in the soma and main processes of astrocytes, which is another hallmark of reactive astrogliosis. Immunostaining and immunoblot showed that treatment with ethyl pyruvate (10 or 15 mM) significantly inhibited the up-regulation of GFAP and vimentin in reactive astrocytes (Figure 3B–D). Additionally, treatment of reactive astrocytes with ethyl pyruvate (10 or 15 mM) also resulted in a significant decrease in their proliferation ability proximate to the scratching injury site (Figure 3E and F), but did not significantly change the extent of cell death (evaluated by measuring LDH activity in the culture medium; data not shown).

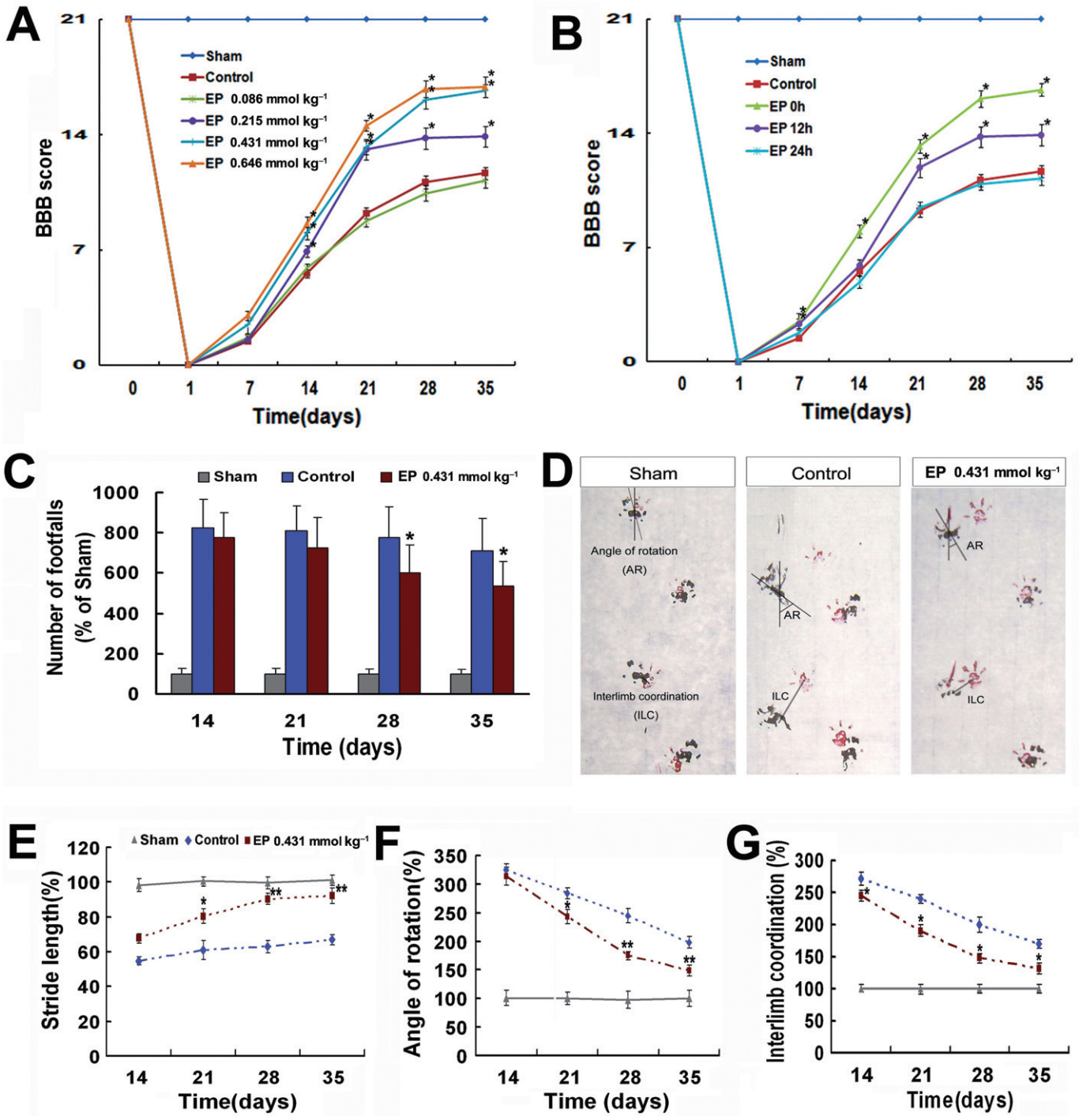

Figure 1

Functional analyses of hindlimb movements. (A) EP (0.086, 0.215, 0.431 or 0.646 mmol·kg^{-1}day^{-1}) was administered i.p. immediately after SCI, then the locomotor BBB score of rats was assessed ($n = 5$ for sham-operated group, $n = 8$ for control group and ethyl pyruvate group, respectively). (B) Analyses of motor function of rats that received ethyl pyruvate (0.431 mmol·kg^{-1}day^{-1}) at 0, 12 or 24 h after SCI. (C) By grid-walk analyses, fewer errors in hindlimb placements were observed in animals treated with ethyl pyruvate at 4 weeks after injury compared with the control groups ($n = 5$ for sham-operated group, $n = 6$ for control group and $n = 7$ for ethyl pyruvate group). (D) Representative footprints of sham, control, and ethyl pyruvate rats ($n = 5$ for sham-operated group, $n = 6$ for control group and $n = 7$ for ethyl pyruvate group) showed improvement in stride length, AR and ILC in the ethyl pyruvate group. (E–G) Quantitative analyses of foot-print revealed that ethyl pyruvate significantly reduced the hindlimb angle of rotation at 3 weeks after SCI and improved stride length and interlimb coordination at 3 and 2 weeks after SCI respectively. *$P < 0.05$, **$P < 0.01$ versus control.

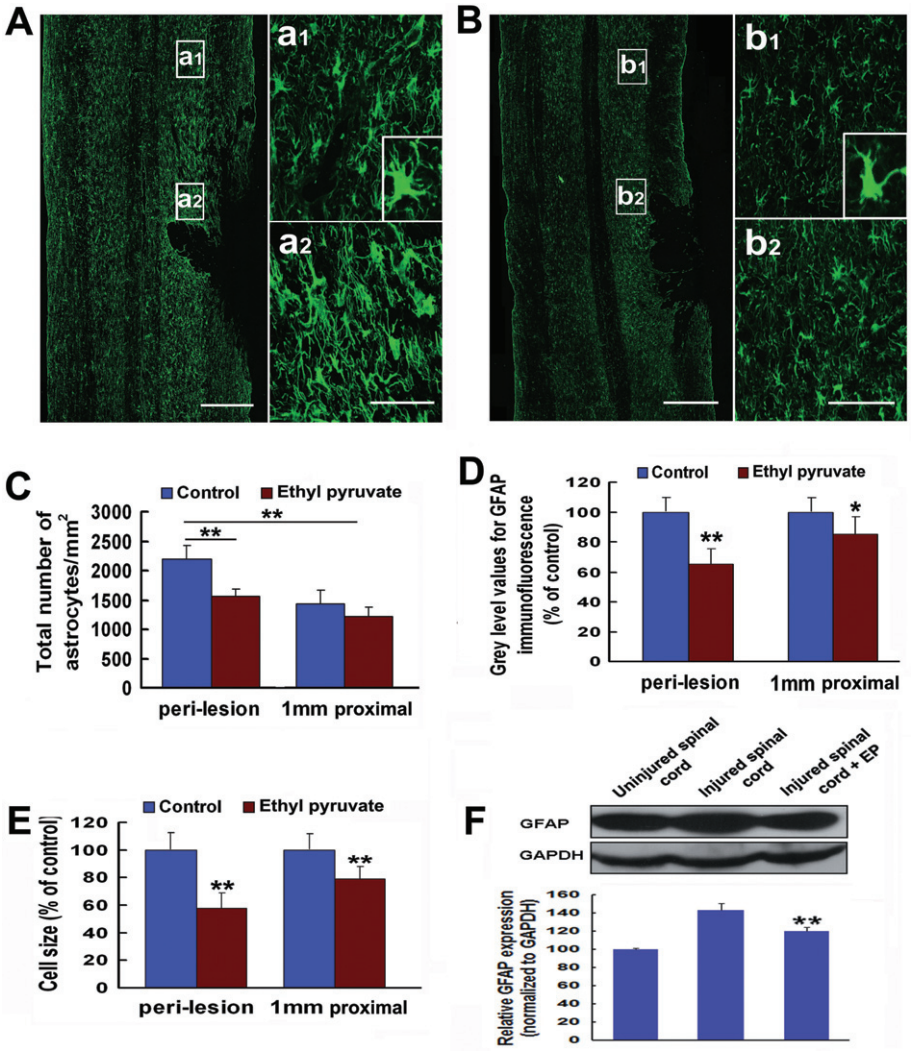

Figure 2

Quantitative assessment of reactive astrogliosis in the damaged spinal cord. (A, B) Effects of ethyl pryuvate on astrocytic gliosis were histologically analysed by immunostaining with GFAP 10 days after treatment of SCI rats with ethyl pyruvate (0.431 mmol·kg^{-1} day^{-1}) (A) or normal saline (B) (n = 6 for control group and ethyl pyruvate group respectively). Insets indicate the reactive astrocyte that was revealed to be hypertrophic under higher magnification. Scale bars: 300 μm in left panel; 100 μm in right panel. (C–E) Quantitative analyses of reactive astrogliosis in the injured spinal cord, including the number, the grey-level value, and the size of GFAP-positive astrocytes close to the lesion site or 1 mm proximal to the lesion site. *P < 0.01 versus control, **P < 0.01 versus control. (F) Western blot analyses of GFAP expression in spinal cord. **P < 0.01 versus injured spinal cord.

A range of physiological changes, including secretion of a variety of cytokines and production of cell adhesion and extracellular matrix molecules, are reported to accompany the morphological changes of reactive astrogliosis. Among these products, CSPG is the main inhibitory component of the glial scar. A decrease in the amount of CSPG deposited is beneficial to axonal regeneration. As shown in Figure 4A, immunostaining for CSPG revealed that the expression of CSPG was markedly reduced in the spinal cord of rats treated with ethyl pyruvate (0.431 mmol·kg^{-1} day^{-1}) compared with that treated with normal saline. To quantify the formation of glial scar, the size of the CSPG immunoreactive area and the intensity of expression of CSPG were measured. Figure 4B and C showed that treatment with ethyl pyruvate greatly decreased the size of the glial scar and CSPG immunoreactivity. Thus, ethyl pyruvate inhibited reactive astrogliosis and ultimately diminished the formation of glial scar *in vivo*.

Ethyl pyruvate alleviates SCI-induced neuroinflammation and promotes neuron survival

Ethyl pyruvate has been reported to act as an ROS scavenger and possess anti-inflammatory and cytoprotective actions (Kao and Fink, 2010). To determine whether ethyl pyruvate affected SCI-induced neuroinflammation, an analyses of macrophage-microglia activation in the damaged spinal cord was performed by staining for CD11b, Iba-1 and ED-1. Ethyl pyruvate (0.431 mmol·kg^{-1}day^{-1}) reduced the infiltration of

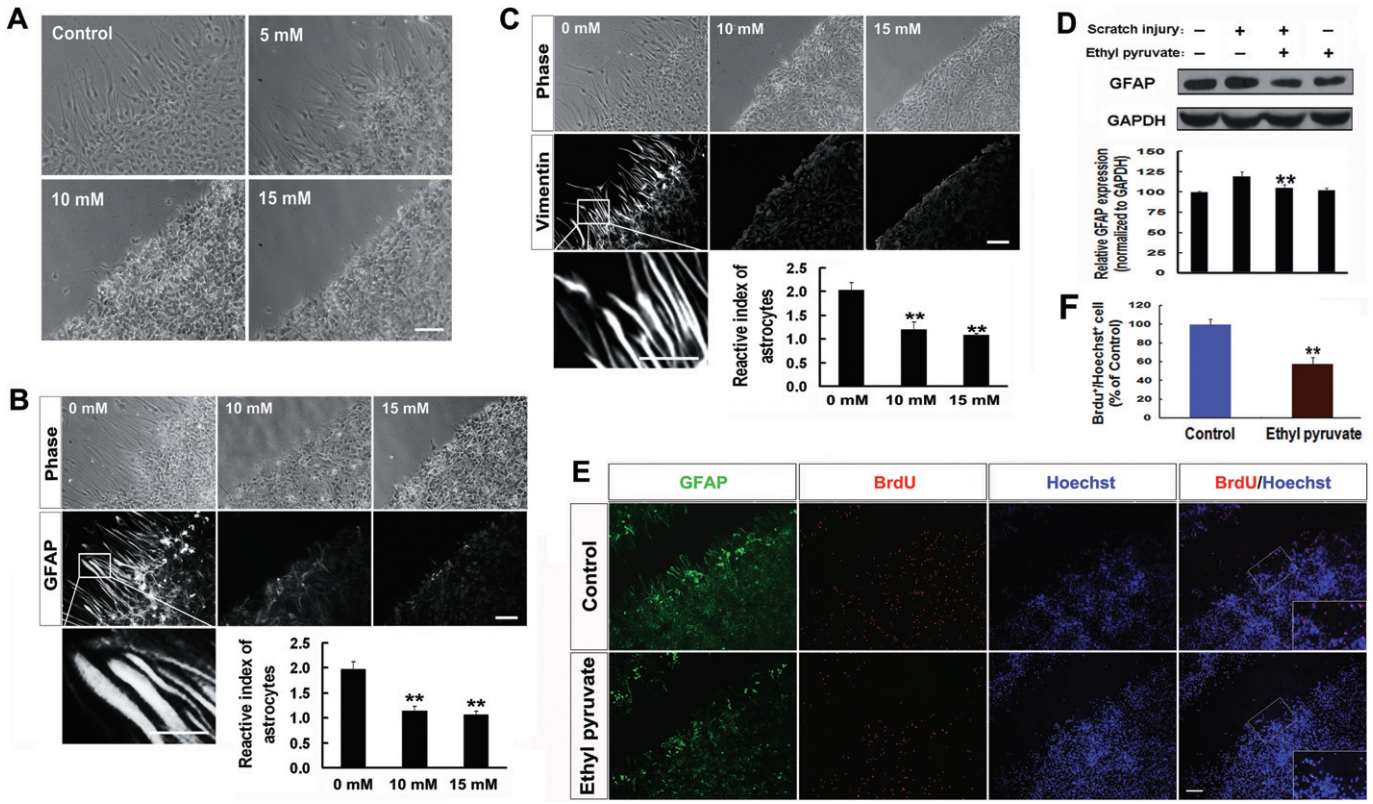

Figure 3

Inhibition of reactive astrogliosis by ethyl pyruvate *in vitro*. (A) The morphological change of astrocytes was observed within the scratch area in presence of ethyl pyruvate (0, 5, 10, 15 mM). Immediately after scratch, ethyl pyruvate at indicated concentration was added to the lesioned cultures of astrocyte. Twenty-four hours later, ethyl pyruvate was shown to inhibit the extensive hypertrophy of cell bodies and cytoplasmic processes of astrocytes proximal to injury; an effect which was dose-dependent. (B, C) Immunocytochemical analysis of GFAP and vimentin expression in scratch injury-induced reactive astrocytes in the absence or presence of ethyl pyruvate (10 or 15 mM). A reactive index of astrocytes, described as a ratio of the average fluorescent intensity of GFAP or vimentin in a narrow zone (150 μm wide) next to the scratch injury to that in another narrow zone (150 μm wide) adjacent to it, was used to quantitatively assess scratch-induced reactive astrogliosis. A reactive index of >1 represents the activation of astrocytes next to scratch injury. The histogram illustrates that ethyl pyruvate significantly inhibited astrogliosis. (D) Effect of ethyl pyruvate on GFAP expression in the scratch injury-reactive astrocytes was analysed by Western blot. (E, F) Ethyl pyruvate inhibited the proliferation of reactive astrocytes in the scratch injury model. Using BrdU labelling, proliferation of astrocytes was examined in the scratch injury model in the absence or presence of 10 mM ethyl pyruvate (E). Insets indicate the BrdU-positive astrocytes under higher magnification. Quantitative assessment of BrdU-positive astrocytes proximate to the lesion induced by scratch (F). $^{**}P < 0.01$ versus control (0 mM). Scale bar = 50 μm.

monocytes/macrophages at the lesion site in terms of the immunoreactivity of CD11b in the injured spinal cord (Figure 5A and D). Figure 5B and E reveal that animals treated with ethyl pyruvate had a significant decrease in the number of activated microglia (Iba-1 immunoreactive cells) in peri-lesion areas, suggesting that SCI-induced microglial activation was inhibited by ethyl pyruvate. The decrease in the number of ED-1 immunoreactive cells in peri-lesion areas was also observed in the rats treated with ethyl pyruvate (Figure 5C and F). These results indicate that ethyl pyruvate exerts an inhibitory effect on the SCI-induced inflammatory response.

The inflammatory response is thought to be important for secondary damage following SCI, resulting in neuronal and glial apoptosis. To examine the effect of ethyl pyruvate on neuron survival in the damaged spinal cord, TUNEL staining was carried out. As shown in Figure 6, treatment of animals with ethyl pyruvate (0.431 mmol·kg^{-1}day^{-1}) significantly decreased the number of apoptotic neurons at the lesion site of spinal cord, indicative of a neuroprotective action of ethyl pyruvate against SCI.

Ethyl pyruvate treatment promotes axonal regeneration across the lesion site

After SCI, axonal survival and regeneration is required for functional recovery. To test whether the ethyl pyruvate-mediated improvement of glial microenvironment at the lesion site contributes to axonal regeneration, an anterograde tracing technique was used to assess the regeneration of CSTs 8 weeks after spinal cord hemisection. In sham-operated animals, equivalent labelling of descending axonal pathways was observed ipsilateral and contralateral to the lesion site (Figure 7B). As shown in Figure 7C, little regeneration of the transected corticospinal axons that are labelled by BDA at

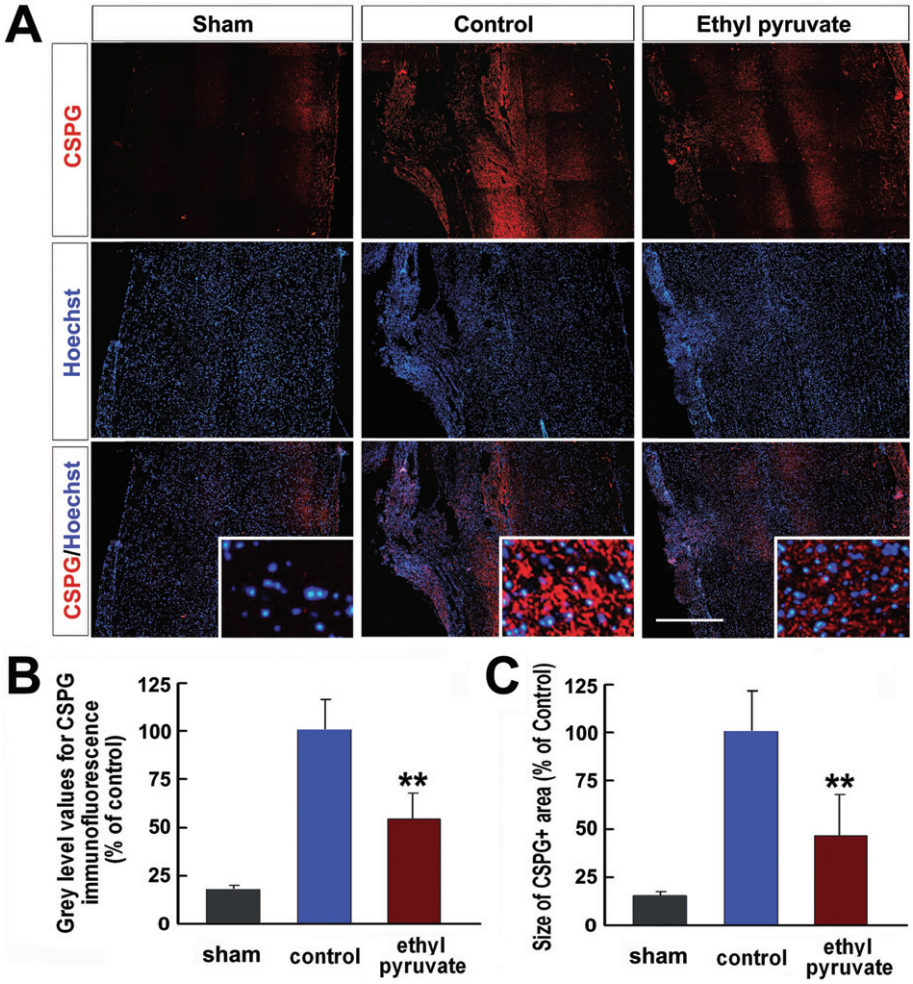

Figure 4

Quantitative analyses of the glial scar formation after SCI. (A) SCI animals were treated with ethyl pyruvate (0.431 mmol·kg^{-1} day^{-1}). Four weeks after SCI, glial scar formation was evaluated by immunostaining for CSPG in horizontal sections through the spinal cord with the lesion epicentre in the middle ($n = 4$ for sham-operated group, $n = 5$ for control group and $n = 4$ for ethyl pyruvate group). Insets indicate the image under higher magnification. (B) Quantitative assessment of the size and immunoreactivity of the CSPG-positive area. $^{**}P < 0.01$ versus control. Scale bar = 400 μm.

0.5 cm caudal to the lesion site was found in the control group. However, treatment of animals with ethyl pyruvate (0.431 mmol·kg^{-1} day^{-1}) resulted in an increase in the number of corticospinal fibres that had grown through the lesion site and reached the segment distal to the lesion epicentre (Figure 7D). For quantitative analyses, regenerating BDA-positive fibres were counted on the sagittal sections 0.5 cm distal to the centre of the lesion site, in term of numbers of BDA-labelled fibres in the segment ipsilateral to lesion site, which was normalized to that in the segment contralateral to the lesion site. Statistical analyses revealed more regenerating BDA+ axons in animals receiving ethyl pyruvate than that in control animals (Figure 7E).

Discussion

The glial cells, including astrocytes, oligodendrocytes and microglia, constitute a neural microenvironment for neurons in the CNS. Besides providing a variety of critical structural and physiological supportive functions that maintain neuronal homeostasis, they also respond to CNS injury or disease (Barres, 2008; Ndubaku and de Bellard, 2008; Aamodt, 2007). For example, astrocytes are complex, highly differentiated cells that tile the entire CNS in a contiguous fashion and make numerous essential contributions to normal function in the healthy CNS, including neurotransmitter regulation, ion homeostasis, blood brain barrier maintenance, and the production of extracellular matrix molecules destined for the basal lamina and perineuronal net (Wang and Bordey, 2008; Sofroniew and Vinters, 2010). However, they become reactive in response to various types of injury, resulting in the formation of the histologically apparent glial scar in damaged CNS (Fitch and Silver, 2008; Sofroniew, 2009). Microglial cells, the resident immune system phagocytic cells within the brain and spinal cord, are usually present in a resting state in the healthy CNS but readily become activated in response to injury, infection, and a variety of neuroinflammatory stimuli

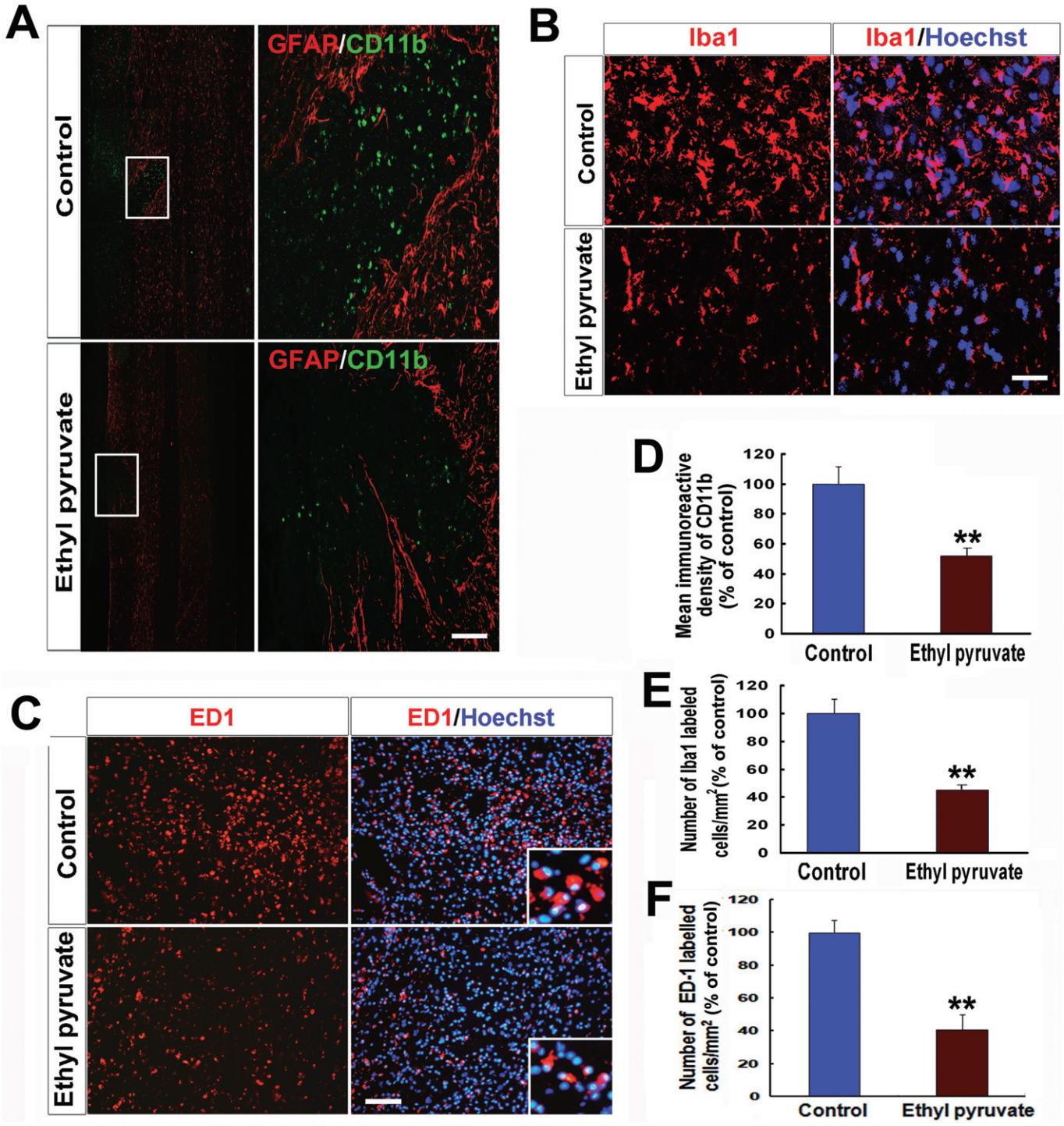

Figure 5

Alleviation of SCI-induced neuroinflammation by ethyl pyruvate at 7 days after injury. (A-C) CD11b, Iba-1 or ED-1 was double stained with GFAP or hoechst at the lesion site of spinal cord after treatment with normal saline (control) or ethyl pyruvate (0.431 mmol·kg^{-1} day^{-1}). (D-F) SCI-induced neuroinflammation was quantitatively assessed by determining the mean immunoreactive density of CD11b at the lesion site and the number of Iba-1 or ED-1 immunoreactive cells in peri-lesion areas ($n = 6$ for control group and $n = 7$ for ethyl pyruvate group). The data of ethyl pyruvate group were normalized to that of control group. Scale bar: 100 μm in (A) and (C); 50 μm in (B). $^{**}P < 0.01$ versus control.

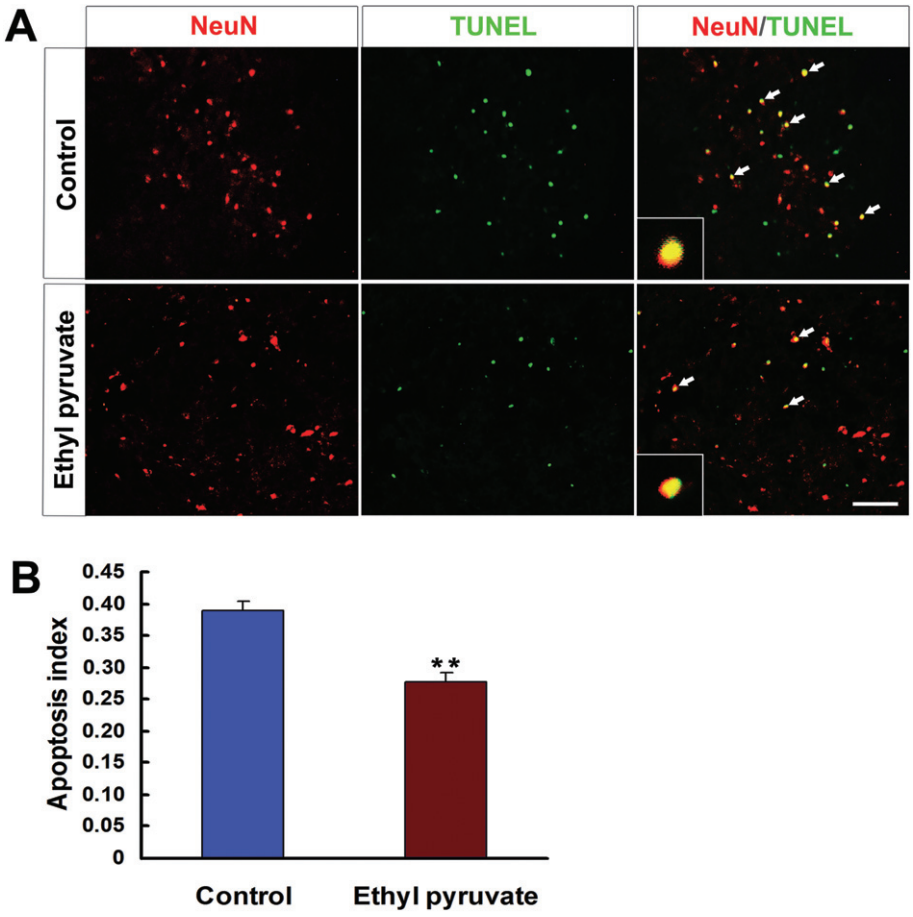

Figure 6

Effect of ethyl pyruvate on neuron survival in the damaged spinal cord. (A) TUNEL labelling of apoptotic nuclei adjacent to the spinal cord hemisection site 24 h after treatment of animals with normal saline (control) or ethyl pyruvate (0.431 mmol·kg^{-1}day^{-1}). Neurons were identified by staining for NeuN. Insets indicate the apoptotic neurons (NeuN$^+$/TUNEL$^+$) under higher magnification. (B) The number of NeuN$^+$/TUNEL$^+$ cells was normalized to the total number of NeuN$^+$ cells (apoptosis index). The bar graph indicates that ethyl pyruvate significantly inhibited the apoptosis of neurons in the damaged spinal cord ($n = 4$ for control group and ethyl pyruvate group respectively). Scale bar = 75 μm; $^{**}P < 0.01$ versus control.

(Kim and de Vellis, 2005; Graeber and Streit, 2010). Glial cell response induced by injuries may result in the formation of a degenerative microenvironment at the lesion site. This hostile microenvironment is implicated as an important factor that leads to the failure of neural regeneration and functional recovery after CNS lesion. In the present study, we showed that treatment of spinal cord-hemisectioned rats with ethyl pyruvate improved the glial microenvironment by attenuating reactive astrogliosis and neuroinflammation and promoting axon regeneration and functional recovery.

Reactive astrogliosis, whereby astrocytes undergo a variety of morphological and molecular changes, including loss of the polarized expression of endfeet proteins, hyperplasia, hypertrophy and up-regulation of intermediate filaments, and secretion of CSPGs, is a ubiquitous hallmark of all CNS pathologies (Sofroniew, 2009; Robel *et al.*, 2011). In severe CNS injury, the reactive astrogliosis ultimately results in the formation of glial scar around the lesion site. Although the scar tissue is required in the acute phase after injury for sealing and cleaning the injury and restoring homeostasis (Okada *et al.*, 2006; Herrmann *et al.*, 2008; Rolls *et al.*, 2009), long-term and/or excessive scar tissue formation is deleterious to functional recovery by constituting a physical and chemical obstacle to axonal regeneration and extension (Widestrand *et al.*, 2007; Sofroniew and Vinters, 2010). Some experimental strategies that modify the astroglial microenvironment in damaged spinal cord, including ablation of proliferating scar-forming astroctyes and knockout or knockdown of molecules produced by reactive astrocytes, have been shown to improve axonal regeneration and functional recovery after injury (Goldshmit *et al.*, 2004; Wilhelmsson *et al.*, 2004; Tian *et al.*, 2006; 2007). In the present study, we demonstrated that astroglial hypertrophy, hyperplasia and GFAP expression were significantly attenuated after treatment with ethyl pyruvate in the spinal cord hemisection model. Moreover, immunostaining for CSPG indicated that the inhibition of reactive astrogliosis resulted in a significant decrease in the formation of the glial scar after SCI. In the *in vitro* cell scratch injury model, ethyl pyruvate was also shown to inhibit the astrocytic proliferation, the

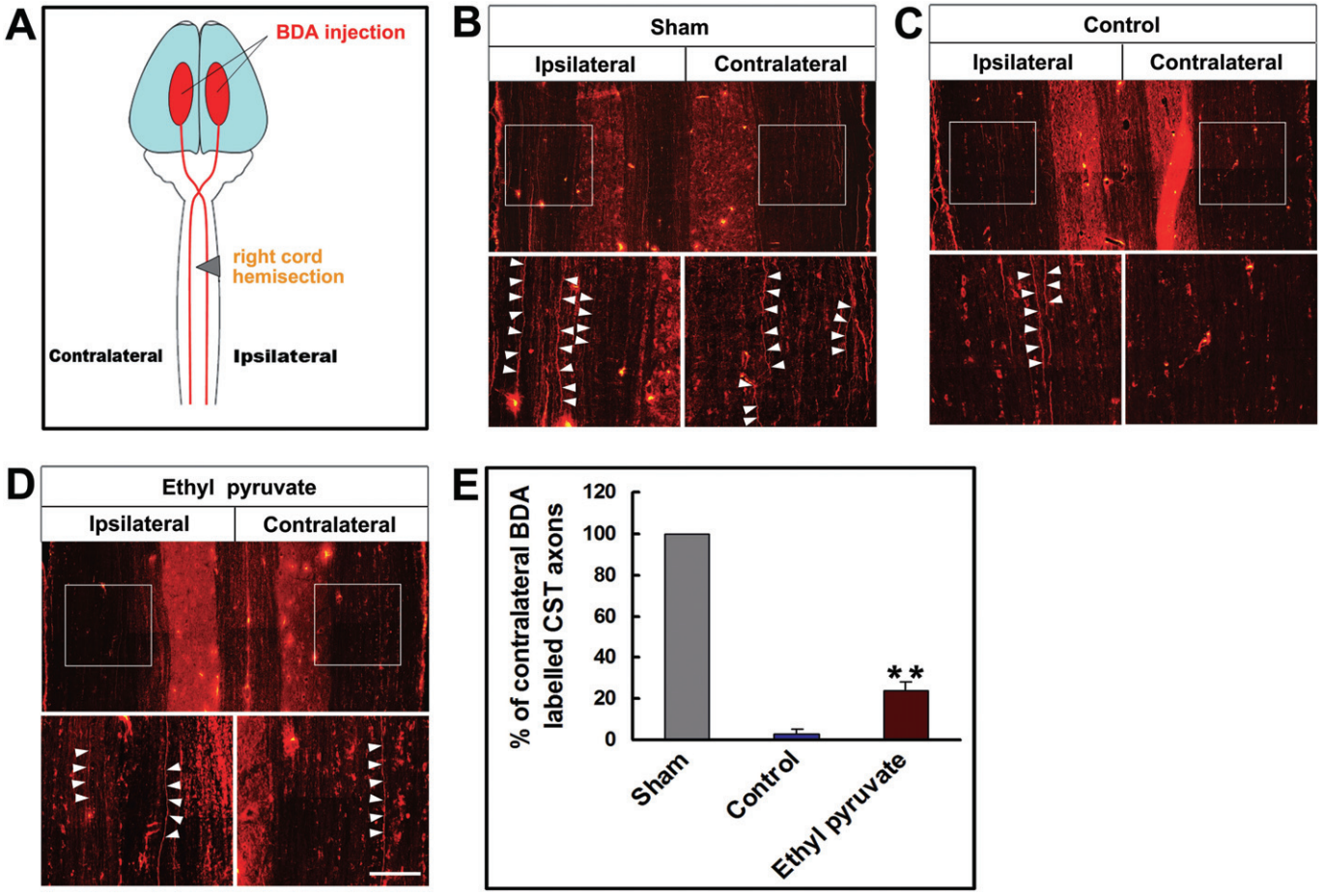

Figure 7

BDA tracing for corticospinal fibres in the animals 8 weeks after SCI. (A) Schematic diagram of BDA anterograde tracing. Hemisection was made at T8 on the right half of the spinal cord, and BDA was injected into the sensorimotor cortex to label endogenous CST. (B–D) Representative photomicrograph of BDA-labelled anterograde corticospinal fibres in horizontal spinal cord section 1 mm caudal to the lesion site. Arrowheads indicate BDA-labelled axons. In the ethyl pyruvate group, SCI rats were injected with 0.431 mmol·kg^{-1}day^{-1}. (E) Quantification of numbers of regenerating BDA^{+} axons in right (ipsilateral to the lesion site) versus left (contralateral to lesion site) half spinal cord among animal groups ($n = 4$ for sham-operated group, $n = 6$ for control group and $n = 5$ for ethyl pyruvate group). Scale bars = 150 μm. $^{**}P < 0.01$ versus control.

hypertrophy of astrocytic processes and the up-regulation of intermediate filament (GFAP and vimentin). However, the difference between effective concentration of ethyl pyruvate *in vitro* (10 mM) and *in vivo* (0.431 mmol·kg^{-1}) should be noted. This discrepancy might suggest that the inhibitory activity of ethyl pyruvate on reactive astrogliosis in the damaged spinal cord is indirect.

Microglial cells are the first cells to be activated, rapidly migrating to the lesion site and initiating a robust neruoinflammatory response by communicating with the immune system (Hanisch and Kettenmann, 2007). The activation of CNS resident microglia and recruitment of blood-born inflammatory cells is thought to trigger a further glial reaction, resulting in secondary tissue damage. Attenuation of the early inflammatory response to SCI may therefore limit the excessive astrogliosis and the extent of tissue injury, and accordingly improve locomotor function (Gris *et al.*, 2004; Cuzzocrea *et al.*, 2008; Tian *et al.*, 2009). As a stable derivative of pyruvate, ethyl pyruvate has recently been documented to have a potential anti-inflammtory and cytoprotective action (Kao and Fink, 2010). For example, ethyl pyruvate is an effective scavenger of hydrogen peroxide and other ROS (Kim *et al.*, 2005; Fink, 2007). Importantly, ethyl pyruvate inhibits many neurotoxic and pro-inflammatory cytokines produced by activated microglia, including COX-2, TNF-α, IL-1β and IL-6 (Kim *et al.*, 2005; 2008). In addition, ethyl pyruvate has also been shown to exert neuroprotective effects on brain energy metabolism (Tokumaru *et al.*, 2009). In the present study, we showed that treatment of animals with ethyl pyruvate resulted in a decrease in both activated microglia and CD11b-positive inflammatory cells in the damaged spinal cord, suggestive of a suppressive effect of ethyl pyruvate on SCI-induced neuroinflammation. Importantly, the TUNEL staining revealed that a comparatively small number of apoptotic neurons were present around the lesion site in ethyl pyruvate-treated rats, indicating that ethyl pyruvate can protect spinal cord neurons from inflammation-mediated damage.

Although ethyl pyruvate evoked a significant amelioration of the abnormal glial microenvironment in the damaged spinal cord, the underlying mechanism of action of ethyl pyruvate was not resolved. Pyruvate, the anionic form of a simple alpha-keto acid, is an effective scavenger of hydrogen peroxide and other ROS as well as an important metabolic intermediate. Although pharmacological administration of pyruvate was shown to improve organ function in animal models of oxidant-mediated cellular injury, the therapeutic potential of this compound might be limited due to its poor stability in aqueous solution. Sims and colleagues developed a more stable aqueous form of pyruvate, ethyl pyruvate (Sims *et al.*, 2001). Ethyl pyruvate is cleaved into ethanol and pyruvate by intracellular esterase in the cytosol (Zeng *et al.*, 2007). Therefore, ethyl pyruvate is proposed to mimic the pluripotent pharmacological effects of pyruvate, including down-regulation of the secretion of pro-inflammatory cytokines, amelioration of redox-mediated damage to cells and tissues, inhibition of apoptosis, and support of cellular ATP synthesis (Kao and Fink, 2010). Despite the firmly established notion that ethyl pyruvate is an effective anti-inflammatory agent, the underlying biochemical mechanisms are still not understood. Song *et al.* showed that ethyl pyruvate exerted anti-inflammatory effects by modifying intracellular glutathione levels and inhibiting NF-κB-dependent pro-inflammatory signalling (Song *et al.*, 2004; Han *et al.*, 2005). Recently, ethyl pyruvate was shown to inhibit the JAK-STAT signalling pathway in activated microglia by Rac1 inactivation or SOCS1 induction (Kim *et al.*, 2008). Because the JAK-STAT signalling pathway also provides astrocytes with a vital mechanism for responding to various extracellular stimuli (Sriram *et al.*, 2004; Schubert *et al.*, 2005; Okada *et al.*, 2006; Herrmann *et al.*, 2008), further study is necessary to determined whether this signalling pathway is also involved in the inhibitory effect of ethyl pyruvate on reactive astrogliosis.

Besides contributing to the intrinsic incapacity of the neuronal regeneration, the hostile glial environment formed at the lesion site is also one of the factors that prevents spontaneous anatomical and functional recovery after SCI. As described above, the glial microenvironment was ameliorated by treatment with ethyl pyruvate. Importantly, BDA anterograde tracing revealed that more nerve fibres were observed regrowing across the lesion site in the animals treated with ethyl pyruvate. The regenerative axons were mirrored by improved locomotor performance assessed by BBB scoring, grid-walk test and foot-print analyses. All these data indicate that ethyl pyruvate-induced amelioration of the glial microenvironment, including inhibition of astrogliosis and attenuation of the inflammatory response, contribute to the axonal regeneration and functional recovery, suggestive of its potential therapeutic benefit for SCI.

Acknowledgements

This work was supported by the National Key Basic Research Program (2011CB504401), National Natural Science Foundation (31171124, 31070922, 31000484), and Shanghai Natural Science Foundation (10ZR1437700).

Conflict of interest

No competing financial interests exist.

References

Aamodt S (2007). Focus on glia and disease. Nat Neurosci 10: 1349.

Barres BA (2008). The mystery and magic of glia: a perspective on their roles in health and disease. Neuron 60: 430–440.

Basso DM, Beattie MS, Bresnahan JC (1995). A sensitive and reliable locomotor rating scale for open field testing in rats. J Neurotrauma 12: 1–21.

Cao L, Liu L, Chen ZY, Wang LM, Ye JL, Qiu HY *et al.* (2004). Olfactory ensheathing cells genetically modified to secrete GDNF to promote spinal cord repair. Brain 127: 535–549.

Cao L, Zhu YL, Su ZD, Lv BL, Huang ZH, Mu LF *et al.* (2007). Olfactory ensheathing cells promote migration of Schwann cells by secreted nerve growth factor. Glia 55: 897–904.

Choi JS, Lee MS, Jeong JW (2010). Ethyl pyruvate has a neuroprotective effect through activation of extracellular signal-regulated kinase in Parkinson's disease model. Biochem Biophys Res Commun 394: 854–858.

Cuzzocrea S, Genovese T, Mazzon E, Esposito E, Di Paola R, Muià C (2008). Effect of 17beta-estradiol on signal transduction pathways and secondary damage in experimental spinal cord trauma. Shock 29: 362–371.

Das UN (2006). Pyruvate is an endogenous anti-inflammatory and anti-oxidant molecule. Med Sci Monit 12: RA79–RA84.

Dusart I, Schwab ME (1993). Secondary cell death and the inflammatory reaction after dorsal hemisection of the rat spinal cord. Eur J Neurosci 6: 712–724.

Fink MP (2003). Ethyl pyruvate: a novel anti-inflammatory agent. Crit Care Med 31 (Suppl. 1): S51–S56.

Fink MP (2007). Ethyl pyruvate: a novel anti-inflammatory agent. J Intern Med 261: 349–362.

Fitch MT, Silver J (2008). CNS injury, glial scars, and inflammation: inhibitory extracellular matrices and regeneration failure. Exp Neurol 209: 294–301.

Fleming JC, Norenberg MD, Ramsay DA, Dekaban GA, Marcillo AE, Saenz AD *et al.* (2006). The cellular inflammatory response in human spinal cords after injury. Brain 129: 3249–3269.

Goldshmit Y, Galea MP, Wise G, Bartlett PF, Turnley AM (2004). Axonal regeneration and lack of astrocytic gliosis in EphA4-deficient mice. J Neurosci 24: 10064–10073.

Graeber MB, Streit WJ (2010). Microglia: biology and pathology. Acta Neuropathol 119: 89–105.

Gris D, Marsh DR, Oatway MA, Chen Y, Hamilton EF, Dekaban GA *et al.* (2004). Transient blockade of the CD11d/CD18 integrin reduces secondary damage after spinal cord injury, improving sensory, autonomic, and motor function. J Neurosci 24: 4043–4051.

Gupta SK, Rastogi S, Prakash J, Joshi S, Gupta YK, Awor L *et al.* (2000). Antiinflammatory activity of sodium pyruvate – a physiological antioxidant. Indian J Physiol Pharmacol 44: 101–104.

Han Y, Englert JA, Yang R, Delude RL, Fink MP (2005). Ethyl pyruvate inhibits nuclear factor-kappaB-dependent signaling by directly targeting p65. J Pharmacol Exp Ther 312: 1097–1105.

Hanisch UK, Kettenmann H (2007). Microglia: active sensor and versatile effector cells in the normal and pathologic brain. Nat Neurosci 10: 1387–1394.

Herrmann JE, Imura T, Song B, Qi J, Ao Y, Nguyen TK *et al.* (2008). STAT3 is a critical regulator of astrogliosis and scar formation after spinal cord injury. J Neurosci 28: 7231–7243.

Hinoi E, Takarada T, Tsuchihashi Y, Fujimori S, Moriguchi N, Wang L *et al.* (2006). A molecular mechanism of pyruvate protection against cytotoxicity of reactive oxygen species in osteoblasts. Mol Pharmacol 70: 925–935.

Huh SH, Chung YC, Piao Y, Jin MY, Son HJ, Yoon NS *et al.* (2011). Ethyl pyruvate rescues nigrostriatal dopaminergic neurons by regulating glial activation in a mouse model of Parkinson's disease. J Immunol 187: 960–969.

Jagtap JC, Chandele A, Chopde BA, Shastry P (2003). Sodium pyruvate protects against $H_{(2)}O_{(2)}$ mediated apoptosis in human neuroblastoma cell line-SK-NMC. J Chem Neuroanat 26: 109–118.

Kao KK, Fink MP (2010). The biochemical basis for the anti-inflammatory and cytoprotective actions of ethyl pyruvate and related compounds. Biochem Pharmacol 80: 151–159.

Karimi-Abdolrezaee S, Eftekharpour E, Wang J, Morshead CM, Fehlings MG (2006). Delayed transplantation of adult neural precursor cells promotes remyelination and functional neurological recovery after spinal cord injury. J Neurosci 26: 3377–3389.

Kim HS, Cho IH, Kim JE, Shin YJ, Jeon JH, Kim Y *et al.* (2008). Ethyl pyruvate has an anti-inflammatory effect by inhibiting ROS-dependent STAT signaling in activated microglia. Free Radic Biol Med 45: 950–963.

Kim JB, Yu YM, Kim SW, Lee JK (2005). Anti-inflammatory mechanism is involved in ethyl pyruvate-mediated efficacious neuroprotection in the postischemic brain. Brain Res 1060: 188–192.

Kim SU, de Vellis J (2005). Microglia in health and disease. J Neurosci Res 81: 302–313.

von Korff RW (1964). Pyruvate-C14, purity and stability. Anal Biochem 8: 171–178.

Lee JY, Kim YH, Koh JY (2001). Protection by pyruvate against transient forebrain ischemia in rats. J Neurosci 21: RC171.

Mongan PD, Capacchione J, Fontana JL, West S, Bünger R (2001). Pyruvate improves cerebral metabolism during hemorrhagic shock. Am J Physiol Heart Circ Physiol 281: H854–H864.

Moro N, Sutton RL (2010). Beneficial effects of sodium or ethyl pyruvate after traumatic brain injury in the rat. Exp Neurol 225: 391–401.

Ndubaku U, de Bellard ME (2008). Glial cells: old cells with new twists. Acta Histochem 110: 182–195.

Okada S, Nakamura M, Katoh H, Miyao T, Shimazaki T, Ishii K *et al.* (2006). Conditional ablation of Stat3 or Socs3 discloses a dual role for reactive astrocytes after spinal cord injury. Nat Med 12: 829–834.

Pekny M, Nilsson M (2005). Astrocyte activation and reactive gliosis. Glia 50: 427–434.

Popovich PG, Hickey WF (2001). Bone marrow chimeric rats reveal the unique distribution of resident and recruited macrophages in the contused rat spinal cord. J Neuropathol Exp Neurol 60: 676–685.

Popovich PG, Wei P, Stokes BT (1997). The cellular inflammatory response after spinal cord injury in Sprague–Dawley and Lewis rats. J Comp Neurol 377: 443–464.

Robel S, Berninger B, Götz M (2011). The stem cell potential of glia: lessons from reactive gliosis. Nat Rev Neurosci 12: 88–104.

Rolls A, Shechter R, Schwartz M (2009). The bright side of the glial scar in CNS repair. Nat Rev Neurosci 10: 235–241.

Ruitenberg MJ, Levison DB, Lee SV, Verhaagen J, Harvey AR, Plant GW (2005). NT-3 expression from engineered olfactory ensheathing glia promotes spinal sparing and regeneration. Brain 128: 839–853.

Schnell L, Fearn S, Klassen H, Schwab ME, Perry VH (1999). Acute inflammatory responses to mechanical lesions in the CNS: differences between brain and spinal cord. Eur J Neurosci 11: 3648–3658.

Schubert KO, Naumann T, Schnell O, Zhi Q, Steup A, Hofmann HD *et al.* (2005). Activation of STAT3 signaling in axotomized neurons and reactive astrocytes after fimbria–fornix transaction. Exp Brain Res 165: 520–531.

Shen HX, Hu XM, Liu C, Wang SP, Zhang WT, Gao H *et al.* (2010). Ethyl pyruvate protects against hypoxic-ischemic brain injury via anti-cell death and anti-inflammatory mechanisms. Neurobiol Dis 37: 711–722.

Sims CA, Wattanasirichaigoon S, Menconi MJ, Ajami AM, Fink MP (2001). Ringer's ethyl pyruvate solution ameliorates ischemia/reperfusion induced intestinal mucosal injury in rats. Crit Care Med 29: 1513–1518.

Sofroniew MV (2009). Molecular dissection of reactive astrogliosis and glial scar formation. Trends Neurosci 32: 638–647.

Sofroniew MV, Vinters HV (2010). Astrocytes: biology and pathology. Acta Neuropathol 119: 7–35.

Song M, Kellum JA, Kaldas H, Fink MP (2004). Evidence that glutathione depletion is a mechanism responsible for the anti-inflammatory effects of ethyl pyruvate in cultured LPS-stimulated RAW 264.7 cells. J Pharmacol Exp Ther 308: 307–316.

Sriram K, Benkovic SA, Hebert MA, Miller DB, O'Callaghan JP (2004). Induction of gp130-related cytokines and activation of JAK2/STAT3 pathway in astrocytes precedes up-regulation of glial fibrillary acidic protein in the 1-Methyl-4-phenyl-1,2,3,6-tetrahydropyridine model of neurodegeneration. J Biol Chem 279: 19936–19947.

Stoll G, Jander S, Schroeter M (2002). Detrimental and beneficial effects of injury-induced inflammation and cytokine expression in the nervous system. Adv Exp Med Biol 513: 87–113.

Su ZD, Yuan YM, Cao L, Zhu YL, Gao L, He C (2010). Triptolide promotes spinal cord repair by inhibiting astrogliosis and inflammation. Glia 58: 901–915.

Tederko P, Krasuski M, Kiwerski J, Nyka I, Białoszewski D (2009). Strategies for neuroprotection following spinal cord injury. Ortop Traumatol Rehabil 11: 103–110.

Tian DS, Yu ZY, Xie MJ, Bu BT, Witte OW, Wang W (2006). Suppression of astroglial scar formation and enhanced axonal regeneration associated with functional recovery in a spinal cord injury rat model by the cell cycle inhibitor olomoucine. J Neurosci Res 84: 1053–1063.

Tian DS, Dong Q, Pan DJ, He Y, Yu ZY, Xie MJ *et al.* (2007). Attenuation of astrogliosis by suppressing of microglial proliferation with the cell cycle inhibitor olomoucine in rat spinal cord injury model. Brain Res 1154: 206–214.

Tian DS, Liu JL, Xie MJ, Zhan Y, Qu WS, Yu ZY *et al*. (2009). Tamoxifen attenuates inflammatory-mediated damage and improves functional outcome after spinal cord injury in rats. J Neurochem 109: 1658–1667.

Tokumaru O, Kuroki C, Yoshimura N, Sakamoto T, Takei H, Ogata K *et al*. (2009). Neuroprotective effects of ethyl pyruvate on brain energy metabolism after ischemia-reperfusion injury: a 31P-nuclear magnetic resonance study. Neurochem Res 34: 775–785.

Vander Heiden MG, Cantley LC, Thompson CB (2009). Understanding the Warburg effect: the metabolic requirements of cell proliferation. Science 324: 1029–1033.

Vavrek R, Girgis J, Tetzlaff W, Hiebert GW, Fouad K (2006). BDNF promotes connections of corticospinal neurons onto spared descending interneurons in spinal cord injured rats. Brain 129: 1534–1545.

Wang DD, Bordey A (2008). The astrocyte odyssey. Prog Neurobiol 86: 342–367.

Wang Q, van Hoecke M, Tang XN, Lee H, Zheng Z, Swanson RA *et al*. (2009). Pyruvate protects against experimental stroke via an anti-inflammatory mechanism. Neurobiol Dis 36: 223–231.

Wang X, Perez E, Liu R, Yan LJ, Mallet RT, Yang SH (2007). Pyruvate protects mitochondria from oxidative stress in human neuroblastoma SK-N-SH cells. Brain Res 1132: 1–9.

Widestrand A, Faijerson J, Wilhelmsson U, Smith PLP, Li L, Sihlbom C *et al*. (2007). Increased neurogenesis and astrogenesis from neural progenitor cells grafted in the hippocampus of GFAP$^{-/-}$ Vim$^{-/-}$ mice. Stem Cells 25: 2619–2627.

Wilhelmsson U, Li L, Pekna M, Berthold CH, Blom S, Eliasson C *et al*. (2004). Absence of glial fibrillary acidic protein and vimentin prevents hypertrophy of astrocytic processes and improves post-traumatic regeneration. J Neurosci 24: 5016–5021.

Yiu G, He ZG (2006). Glial inhibition of CNS axon regeneration. Nat Rev Neurosci 7: 617–627.

Yu ACH, Lee YL, Eng LF (1993). Astrogliosis in culture. I. The model and the effect of antisense oligonucleotides on glial fibrillary acidic protein synthesis. J Neurosci Res 34: 295–303.

Yu YM, Kim JB, Lee KW, Kim SY, Han PL, Lee JK (2005). Inhibition of the cerebral ischemic injury by ethyl pyruvate with a wide therapeutic window. Stroke 36: 2238–2243.

Zeng J, Liu J, Yang GY Kelly MJ, James TL, Litt L (2007). Exogenous ethyl pyruvate versus pyruvate during metabolic recovery after oxidative stress in neonatal rat cerebrocortical slices. Anesthesiology 107: 630–640.